TNFα DEPLETION INDUCES REPRESIVE EPIGENETIC MODIFICATIONS IN DENDRITIC CELLS DURING IMMUNE RESPONSE TO *Cryptococcus neoformans*

Nicole Potchen
April 2016

This thesis has been read and approved by Dr. Michal Olszewski

Signed: Michal Olszewski Date: 04/18/2016

Faculty advisor e-mail: olszewsm@med.umich.edu Phone: (734) 845-5238

Author and Contributor Information

Author

Nicole Potchen

Biochemistry Major, Gender & Health Minor, B.S. 2016
College of Literature Science and the Arts
University of Michigan
npotchen@umich.edu

Mentor

Michal Olszewski, D.V.M. Ph.D.
Co-sponsor and Principal Investigator
Associate Professor
Division of Pulmonary and Critical Care Medicine, Internal Medicine
University of Michigan Medical School
olszewsm@umich.edu

Medical Research Scientist, Research Service (11R)
VA Ann Arbor Health Care System (506)

Research Supervisor

Alison Eastman, B.S., Ph.D. Candidate

Graduate Program in Immunology
University of Michigan Medical School
alisonjeastman@gmail.com

Table of Contents

Abstract

Every year, the fungal pathogen *Cryptococcus neoformans* infects roughly 1 million people and results in over 600,000 deaths worldwide. This opportunistic pathogen is the leading cause of death for patients who are immunocompromised, including individuals with HIV/AIDS. Upon infection with *C. neoformans*, the development of a Th1 immune response is critical for fungal clearance. TNFα, a pro-inflammatory cytokine, has been shown to be critical to the priming of dendritic cells (DCs) that train the appropriate action of T-cells. We explored the mechanism behind the interaction between TNFα and DCs, specifically, to determine if TNFα induces changes on the epigenetic level in DCs. By examining genes critical to the mounting of the Th1 response, we found that depletion of TNFα leads to higher expression of DC2 genes and a more Th2 polarized response. This corresponds to higher levels of global repression, indicated by epigenetic marker H3K27me3, and higher levels of histone methyltransferase EZH2. Because epigenetic modifications are the means by which immune cells "remember" to express or not to express certain genes, we concluded that TNFα plays a critical role in programing DC function during cryptococcal infection. Specifically, our data showed that TNFα prevented repressive epigenetic modifications on DC1 genes, contributing to the "DC1 training" of DCs necessary for induction of the protective T-cell mediated immune response. After analyzing which DC genes were associated with this repressive modification, we found the key DC1 gene IL-12b had been repressed upon depletion of TNFα. Our findings have shed light on the effects of this cytokine in the immune response to *C. neoformans* infection and may have broader implications regarding the mechanisms by which DCs are trained to execute certain type of functional training in hosts upon infection with a variety of pathogens.

Introduction

Cryptococcus neoformans

Every year, *Cryptococcus neoformans* (*C. neo*), an opportunistic fungal pathogen, infects over 1 million people every year and leads to fatality in over 600,000 patients [1]. Currently, *C. neo* is the leading cause of fatal fungal infection among immunodeficient hosts, including people who are infected with HIV/AIDS [2, 3]. *C. neo* is a common environmental yeast found in tree bark and pigeon excreta ; inhalation of spores or desiccated yeast into the lungs is thought to be the route of infection [4-6]. The yeast is able to reproduce by budding and is non-filamentous in hosts [7]. Upon infection, the yeast then lodges in the patient's alveoli, and without a protective immune response, leads to dissemination to the central nervous system (CNS) [8]. Infection with *C. neo* can also be latent or persistent over time, and can cause symptoms of the infection to recur if the immune system becomes compromised [9, 10].

The Immune Response

T-helper cell mediated immunity is required for clearance of *C. neo*. In the absence of a protective immune response, *C. neo* is able to disseminate from the lungs to the CNS, which can result in meningitis and can be fatal to the host [1].

A. The Innate Immune System

Upon infection, the host's innate immune system must decide how the more productive method to proceed to lead to fungal clearance. The exterior surface of the fungal pathogen contains pathogen associated molecular patterns (PAMPs) [11], which can be recognized by various host cells. Many types of cells, including macrophages and dendritic cells (DCs), natural

killer (NK) cells, and neutrophils, are able to recognize these PAMPs by pattern recognition receptors (PRRs) on their surface [12]. Upon recognition of infection of *C. neo*, an immune response is activated.

DCs and macrophages are known as antigen presenting cells (APCs) because they are able to process antigens and present these molecules on their surface. More specifically, DCs are known as "professional APCs" because of their abilities to signal to T-cells and stimulate an adaptive response. DCs express the integrin CD11c on their surface, which is a transmembrane protein that can be used experimentally to identify DC populations [13]. Upon the phagocytosis of *C. neo*, DCs process the pathogen and load the antigen onto major histocompatibility complexes (MHCs), which are then shuttled to the cell surface to be presented to T-cells [14]. MHC molecules are split up into Class I and II depending on which T-cell molecule bind they bind with at a higher affinity (CD8 and CD4 respectively). After phagocytosis of the pathogen, DCs go through a process of maturation and polarization, during which they up-regulate expression of MHC II, surface receptors, co-stimulatory molecules, and cytokines. DCs then migrate to the draining lymph nodes, where these specific "patterns" of cell-bound and soluble signals expressed by DCs directs the development of specific T-cell responses [15].

B. The Adaptive Immune System

Effective clearance of *C. neo* relies on the development of a Th1 type response [16-18]. T-cells can be polarized in a variety of ways to have differential responses, some of which include Th1, Th2, Th17 and T-reg [19]. T-cells producing the cytokines IFNγ, TNFα, or IL-17, known as Th1 and Th17 respectively, are necessary for protective immunity to *C. neo* [17, 18, 20, 21]. Conversely, T-cells producing IL-4, known as a Th2 response, are ineffective for

clearance of the infection [17, 22-25]. Professional APCs, or DCs, are critical for priming the T-cell immune response; DC priming Th1/Th17 responses are termed DC1, while DC priming Th2 responses are DC2. DC1s are characterized by robust iNOS expression, whereas the DC2s that prime a non-protective Th2 response are characterized by expression of Gal3, Fizz1, IL-5 and IL-13[15].

Three signals are necessary for the DC to effectively prime the naïve T-cell [19]. The first is the interaction between the MHC and the T-cell receptor (TCR). This requires the high affinity binding of the TCR and the presence of either glycoprotein CD8 or CD4 from the T-cell with the MHC Class I or II on the DC loaded with an antigen. The second required signal is between co-stimulatory molecules CD40 and CD80/86 on the DC and CD40L and CD28 on the T-cell. Lack of CD40 or CD80/86 on the DC halts the priming and activation of T-cells. The third necessary signal is the cytokines released from the DC, some of which include IL-12, IL-6, TGF-β and IL-4. Higher levels of CD40, CD80/86 and MHCII on DCs are necessary for proper protective T-cell stimulation (reviewed in [26]).

Tumor Necrosis Factor Alpha (TNFα)

The pro-inflammatory cytokine TNFα acts in DCs by signaling through the MAPK and NFKB pathways [27]. Previous experiments have shown that defects in TNFα signaling early during the DC-dependent phase of *C. neo* infection results in non-protective immunity [28-31]. Transient depletion of cytokine TNFα, which is normally produced by the host during protective response to *C. neoformans*, results in a development of non-protective response. These negative effects of early depletion remain even after levels of TNFα recover in about a week post anti-TNFα administration [28-31].

It has been previously established that immunotherapy with antibodies against TNFα used as treatment for rheumatoid arthritis lead to increased burden of a variety of fungal infections [32, 33]. TNFα blockers, including adalimumab, etanercept, and infliximab, are used in humans to treat autoimmune diseases, including rheumatoid arthritis [34]. Adalimumab was approved by the FDA approved in 2002 for rheumatoid arthritis, psoriatic arthritis, ankylosing spondylitis, plaque psoriasis, Crohn's, Ulcerative Colitis, moderate to severe chronic psoriasis, and juvenile idiopathic arthritis [35]. Other TNFα blockers have also been found to treat diseases including ankylosing spondylitis and plaque psoriasis [36]. These TNFα blockers work through a variety of methods, which including blocking the TNFα Receptors (TNFRI and TNFRII), or by blocking soluble and membrane-bound TNFα [34].

Other immunocompromised individuals are highly susceptible to *C. neo* infection because they are not able to make successful TNFα signaling [37]. However, some of the more virulent strains of *C. neo* are able to suppress the TNFα response even in immunocompetent hosts, causing a non-protective immune response and dissemination to the CNS [38].

Epigenetic Modifications

Studies on epigenetic changes to DNA and histone proteins are becoming increasingly popular to explain gene expression. Modifications to histone proteins at the gene promoter region serve as a mechanism by which cells "remember" to express or to not express specific genes [39]. Histone protein complexes are comprised of a clustered group of eight similar protein structures, which DNA can wrap around. They are comprised of two of each of the segments H2A, H2B, H3 and H4, to create an octamer. Each segment has multiple tails that help to control

how tightly DNA is wrapped around the protein structure. These tails contain many positively-charged amino acids, including lysine (K) and arginine (R) in order to adhere to the negatively charged phosphate backbone of DNA (reviewed in [40]).

Various molecules added to the histone tails affect how tightly DNA is wrapped around the histone proteins. For example, acylation of histone proteins creates more space between the DNA and protein, allowing for easier access by transcription factors (TFs) and allows for more gene expression [39]. Methylation can be either inhibitory or activating, depending on where it is deposited. Tri-methylation of Lysine 27 residue on Histone 3 (H3K27me3) is associated with gene repression [41], while similar modification at Lysine 4 residue (H3K4me3) is associated with increased levels of gene expression [42]. Histone methylation status is an outcome of enzymatic activities of methyltransferases and demethylases, responsible for the addition and removal of the methyl groups from histone tails, respectively [43]. EZH2 is a histone methyltransferase enzyme that inhibits gene expression via the addition of a tri-methyl group to H3K27 [44]. Conversely, MLL1 is a histone methyltransferase that facilitates gene activation by adding a tri-methyl group to H3K4 [45]. Enzymes such as EZH2 and MLL1 affect the specific gene promoter regions and have lasting effects on gene expression patterns. These changes to gene expression patters in turn affect translation of proteins critical for execution of specific cell functions [46].

TNFα receptor signaling leading to epigenetic modification is poorly characterized, although some pioneering studies provide evidence of epigenetic signaling. TNFα receptors signal through multiple pathways, including NFKB and MAPK pathways [27]. Signaling through the NFKB pathway is known to lead to MLL1 activity [47]. Similarly, the MAPK pathway influences EZH2 action [48].

In this study, our aim was to determine if TNFα signaling affects the repressive motif H3K27me3 if this contributes to "training" of DCs towards either DC1 or DC2. Because TNFα is associated with a Th1 immune response, we hypothesize that TNFα prevents repressive modification H3K27me3 at DC1 gene promoter regions. Since DC1 or DC2 polarization directly influences the priming of the T-cell response into Th1 or Th2 (protective or non-protective against infection of *C. neo*), a greater understanding of this mechanism could gain insight into potential targets for therapies or treatments.

Materials and Methods

Cryptococcus neoformans

The 52D strain obtained form the American Type Culture Collection (ATCC 24067) of *Cryptococcus neoformans* was used for our experiments. The pathogen was recovered from frozen stocks stored at -80°C with 10% glycerol. It was cultured to log phase at 37°C in Sabouraud dextrose broth (1% neopeptone, 2% dextrose; Difco, Detroit, MI) on a shaker. The cultures were then washed in non-pyrogenic saline (Travenol, Deerfield, IL), counted on a hemocytometer, and diluted to 3.3×10^5 yeast cells/mL in sterile non-pyrogenic saline.

Animals

Female CBA/J Mice obtained from Jackson Laboratories (Bar Harbor, ME) were used for our studies. Mice were housed under pathogen-free conditions and enclosed in filter-top cages. The mice were aged between 8-10 weeks at the time of infection with *Cryptococcus neoformans*, or 12 weeks at the time of bone marrow isolation. Animals were humanely euthanized using CO_2 inhalation. The University Committee on the Use and Care of Animals and the Veterans Administration Institutional Animal Care and Use Committee approved all experiments.

Intratracheal Inoculation

Mice were anesthetized via intraperitoneal injection of Ketamine and Xylazine (100 and 6.8 mg/kg body weight, respectively) and were restrained on a foam plate using tape. A small incision was made through the skin covering the trachea, and the underlying salivary glands and muscles were separated. Infection was performed by intratracheal injection of 30 μL (10^4 CFU)

via 30-gauge needle actuated from a 1-ml tuberculin syringe with *C. neoformans* suspension (3.3 $\times 10^5$ /mL). The skin was then closed with cyanoacrylate adhesive. Mice were monitored, placed under a heat lamp, and given artificial tears during recovery from anesthesia. The animals recovered with minimal visible trauma. Following infection, the inoculum were cultured and plated for CFU (Colony Forming Units) to confirm the number of organisms injected into the mice.

Anti-TNFα Injection

Mice received treatment with either an anti-TNFα antibody (100 ng/mouse, Taconic, Hudson, NY) or non-specific IgG (vehicle) as a control prior to infection with *C. neoformans.* Mice received injections of 20 μL via intra-peritoneal route at day 0.

Lung Leukocyte Isolation

Lungs were perfused free of peripheral blood cells with PBS. The perfused lungs were then excised, washed with RPRMI, minced with scissors, and dissociated by gentleMACS tissue dissociator (Miltenyi Biotec, Cambridge, MA). Dissociated samples were digested enzymatically in an incubator at 37°C for 35 min in 10 mL/mouse of digestion buffer [RPMI, 5% FBS, penicillin and streptomycin (Invitrogen, Grand Island, NY); 1 mg/ml collagenase A (Roche Diagnostics, Indianapolis, IN); and 30 μg/mL DNase (Sigma, St. Louis, MO)], and then dissociated a second time more vigorously. An aliquot of the suspension was then removed for CFU. The samples were then centrifuged and re-suspended with RPMI. The cell suspension and tissue fragments were then further dissociated, centrifuged, and re-suspended with RPMI. Erythrocytes in the cell pellets were lysed by addition of 3 mL NH_4Cl buffer (0.829% NH_4Cl, 0.1% $KHCO_3$, and 0.0372% Na_2EDTA, pH 7.4) for 3 minutes followed by a 10-fold addition of

cold RPMI. Cells were pelleted and re-suspended in RPMI. The cell suspension and tissue fragments were then further dissociated by aspiration through a 10 mL syringe, followed by filtration through a sterile 100-μm nylon screen (Nitex, Kansas City, MO). The filtrate was centrifuged for 30 min at 3000 RPM in the presence of 20% Percoll (Sigma) to separate leukocytes from cell debris and epithelial cells. Leukocyte pellets were re-suspended in 5 mL complete RPMI media, and enumerated on a hemocytometer following dilution in Trypan Blue (Sigma, St. Louis, MO).

Colony-Forming Unit Assay

Spleens were removed from mice and cells were lysed with sterile DI water. For lungs, aliquots were collected during lung leukocyte digest (described above) to determine the fungal burden. 10-fold serial dilutions of each sample were plated on Sabouraud dextrose agar plates in duplicates of 10-μl aliquots. Each plate incubated at room temperature for 3 days. *C. neoformans* colonies were counted 2 days later and the number of colony-forming units (CFU) was calculated on a per-organ basis.

Pulmonary T-cell and Dendritic Cell Isolation

10^8 lung leukocytes from each sample were exposed to a PE labeling reagent, incubated, exposed to EasySep PE Selection Cocktail, and incubated further (Stem Cell, Vancouver, BC). EasySep magnetic nanoparticles were added to attach to $CD4^+$ cells (T-cells) and eluent was poured off. Cells were washed with 2% FBS in PBS 3 times, resuspended in buffer, centrifuged, and resuspended in Trizol. CD11c+ cells (DCs) were then isolated from the eluent via the same procedure, pelleted, and resuspended in Trizol.

Quantitative Real-Time PCR (qRT-PCR)

RNA samples were isolated from Trizol using a phenol chloroform purification. Samples were separated from Trizol followed by purification with isopropanol. RNA was then quantified using a spectrophotometer. A Reverse Transcriptase (RT) reaction was preformed, which generated first-strand cDNA using RNeasy Plus Mini Kit (Invitrogen, Carlsbad, CA) according to the manufacturer's instructions using 500ng total mRNA per sample. qPCR was performed using an MX 3000P system (Stratagene, La Jolla, CA) according to the manufacturer's protocols. Forty cycles of PCR (94°C for 15 seconds followed by 60°C for 30 seconds and 72°C for 30 seconds) were performed on a cDNA template. The mRNA levels were normalized to beta-acctin levels and the ratio of sample to uninfected-baseline expression level (fold induction) was calculated for each sample.

Cytometric Bead Array

Serum was isolated from whole blood, and cytometric bead assays were performed according to the manufacturer’s protocol (BioLegand, San Diego, CA). After staining, the beads were run on an LSRII flow cytometer and analyzed with software provided by manufacturer.

Flow Cytometry

All staining reactions were performed according to the manufacturers' protocols. Data were collected on a FACS LSR II flow cytometer using FACSDiva software (BD Biosciences, San Jose, CA) and analyzed using FlowJo software (Tree Star, San Carlos, CA). 200,000 cells were analyzed per sample at a minimum. Gates were initially set based on light-scatter characteristics (side scatter and forward scatter) followed by gating on $CD45^+$ population, then T-cells were

separated from myeloid cells by expression of CD3, CD4, CD8, CD11b, CD11c. Macrophages were distinguished from DCs by auto-fluorescence and CD11b expression. The total number of cells within each mouse tissue was calculated by multiplying the frequency of this population by the total number of leukocytes in each sample (percentage of cells multiplied by the original hemocytometer count of total cells).

Isolation & Culture of Bone-Marrow Derived Dendritic Cells (BMDCs)

Bone marrow cells were isolated from CBA/J female mice from tibias and femurs and flushed with a 5 mL of DMEM media per bone using a 1 mL syringe and a 25½-guage needle. Media contained DMEM [1g/L glucose + L-Glutamine + 110mg/L sodium pyruvate] 20% FBS, 1x GlutaMAX, 1x MEM nonessential amino acids, 1x sodium pyruvate, 20ng/mL GM-CSF, 100 ug/mL streptomycin, 100 units/mL penicillin. Cells were dissociated by aspiration through a 10 mL syringe, followed by filtration through a sterile 100-µm-nylon screen (Nitex, Kansas City, MO). The cells were then centrifuged, resuspended in the DMEM media and cultured in cells were cultured in 100 × 15-mm dishes at a concentration of 2 x 10^6 cells per dish. After 7 days, the loosely adherent BMDCs were removed and plated at a density of 1 x 10^6 cells/ml in 2 mls in a non-tissue-culture-treated 6-well dish. Cells were exposed to primary cytokine stimulations for 24 hours, washed, and treated secondary cytokine stimulations for a subsequent 24 hours (described in Fig. 3 below). Following these sequences, BMDCs were removed via Trizol and processed for RNA and qRT-PCR.

Chromatin Immunoprecipitation Assay

Cells were fixed in formaldehyde using a final concentration of 2% formaldehyde. Reactions were stopped using 2.5 M glycine. Cells were frozen at -80°C until sufficient numbers for

performing ChIP were collected. Cells were lysed in cell lysis buffer (10 mM Tris-HCl, 10 mM NaCl, 0.2% NP40, 10 mM sodium butyrate, 300 uM PMSF, 1x complete protease inhibitor). Nuclei were pelleted and lysed with nuclear lysis buffer (50 mM Tris-HCl, 10 mM EDTA, 1% SDS, 10 mM sodium butyrate, 300 uM PMSF, 1x complete protease inhibitor). Cells were sonicated on ice with ChIP IP dilution buffer (20 mM Tris-HCl, 2 mM EDTA,150 mM NaCl, 0.01% SDS, 1% Triton X-100, 10 mM sodium butyrate, 300 uM PMSF, 1x complete protease inhibitor). Lysates were pre-cleared using preimmune rabbit serum and immunoprecipitation was performed overnight at 4°C. Antibodies used were H3K27me2me3 (Active Motif, Carlsbad, CA) and control IgG (R&D Systems, Minneapolis, MN). Protein A Agarose beads were added to immunoprecipitate antibody-protein-DNA complexes. Crosslinking was reversed using 5M NaCl overnight at 67°C and nucleic acids were purified using phenol-chloroform extraction. Recovered DNA was analyzed by qPCR using primers specific for the promoter regions of IL-12b gene.

Calculations and statistics

Statistical significance was calculated using Student's t-test for individual paired comparisons or t-test with Bonferoni adjustment, whenever multiple groups were compared. Means with *P*-values of < 0.05 were considered significantly different and were represented by *. P-values of < 0.01 were represented by ** and P-values of < 0.001 were represented by ***. All values are reported as means ± standard errors (SEM). Calculations were performed using Prism of GraphPad software (La Jolla, CA).

Results

Transient TNFα depletion leads to increased chronic fungal burden and higher levels of Th2-associated cytokines.

To determine how TNFα depletion affects fungal clearance, we analyzed fungal burden and Th2 cytokine expression levels. CBA/J mice were infected intratracheally with *Cryptococcus neoformans* strain 52D and either received TNFα blocking antibody (anti-TNFα) or an isotype control antibody injected intraperitoneally at the time of infection. Colony forming units (CFU) from harvested lung and spleen were evaluated for both treatment groups at 1, 2 and 4 weeks post-infection (wpi). TNFα depletion did not change pulmonary fungal burden at week 1, but led to an increased fungal burden in the lung at weeks 2 and 4 (Fig. 1A). Anti-TNFα mice had progressive dissemination to the spleen, while the dissemination in control mice was transient and minimal (Fig. 1B), together suggesting that TNFα is critical early in the immune response for protective clearance of the pathogen, while its absence results in a non-protective response.

Because a switch from the protective Th1 response to a non-protective Th2 could account for the loss of protection that followed transient depletion of TNFα, we next examined involvement of Th2 cytokines. Serum cytokine levels from both treatment groups were evaluated using a cytometric bead array. Mice that recieved anti-TNFα treatment had increased levels of non-protective cytokines IL-13 and IL-5 compared to the control group throughout infection (Figs. 1C-D). This prolonged non-protective immune response marked by elevated systemic levels of Th2 cytokines in the anti-TNFα mice strongly suggests that in the absence of early TNFα signaling, mice deviated to a Th2 –type immune response.

Figure 1

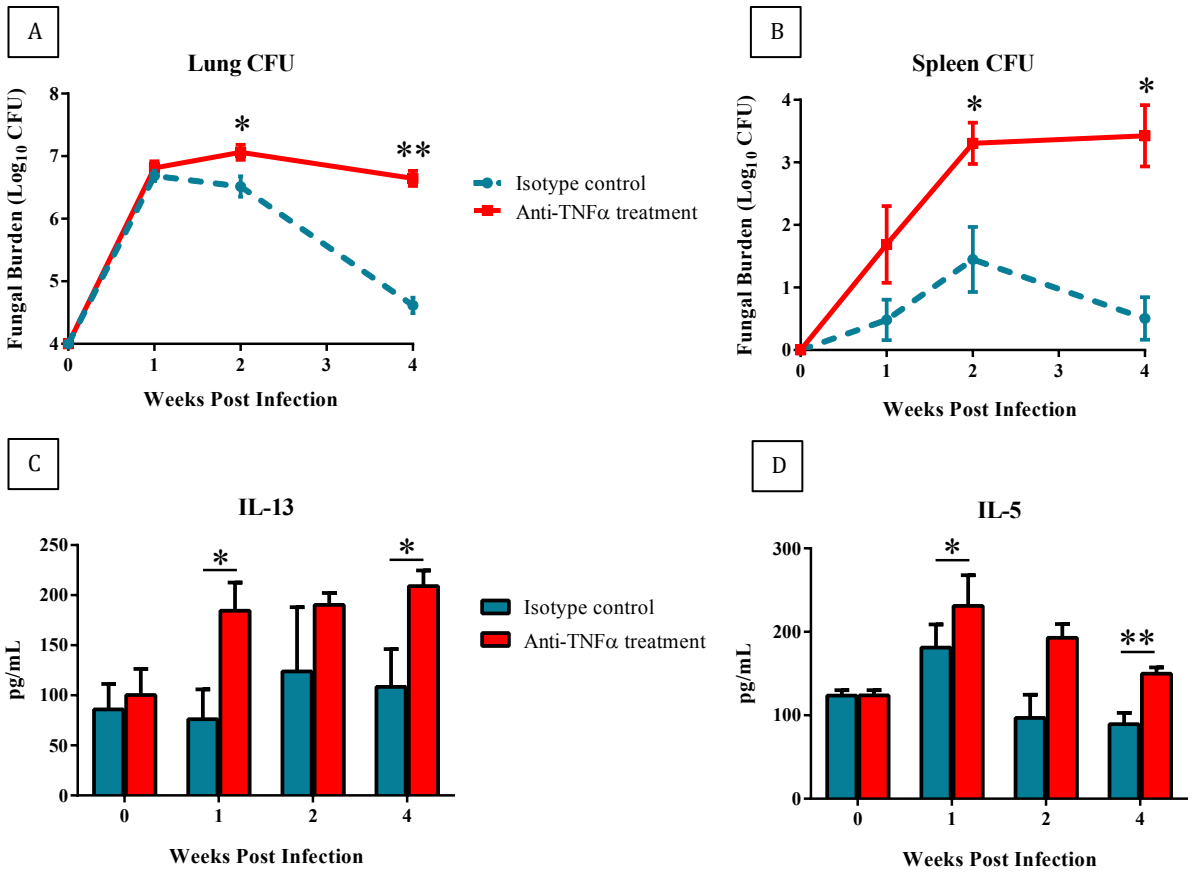

Figure 1 - Mice were infected intratracheally with 10^4 CFU of *C. neoformans*. Harvests were performed at 1, 2 and 4 weeks post infection (wpi). Fungal burden was assessed from harvested lung and spleen from mice treated with isotype control and mice treated with anti-TNFα upon infection (n = 4) (Figs. 1A-B). Cytometric bead arrays were performed using blood serum isolated from CBA/J mice (n = 7) (Figs. 1C-D). Data represent mean pooled from three separate matched experiments. * $p < 0.05$, ** $p < 0.01$ between indicated groups.

Mice depleted of TNFα display a Th2 response, which is preceded by DC2 activation of pulmonary DCs.

To determine if the absence of TNFα signaling resulted in *bona fide* change in T-cell polarization, we assessed how early TNFα depletion affected subsequent CD4 T-cell polarization status in the infected lungs. We analyzed polarization in magnetically separated $CD4^+$ T-cells by measuring mRNA expression of key Th1/Th17 cytokines. T-cells were magnetically separated from lung leukocytes isolated from mice infected with *C. neoformans* that were either TNFα depleted using the blocking antibody or received an isotype control. TNFα depletion led to a decrease in the Th1 master transcription factor T-bet and decreased expression of Th1 and Th17 associated cytokines (IFNγ, IL-17, IL-23) (Fig. 2A). Thus in the absence of TNFα, T-cell polarization is skewed towards the non-protective Th2 polarization at 2 wpi. Because DCs prime T-cells in both the lymph node and the lung, this suggested to us that DCs responsible for T-cell priming may be different in the presence or absence of TNFα. Next, we assessed DC1 and DC2 gene expression from mRNA extracted from $CD11c^+$ cells magnetically isolated from infected mouse lung. Treatment with the TNFα blocking antibody led to decreased levels of DC1 marker iNOS and increased levels of DC2 marker Arginase (Fig. 2B), whereas the control mice had increased iNOS and decreased Arginase expression. To confirm DC1/DC2 polarization at the protein level, we performed flow cytometry on pulmonary DCs isolated from infected lungs at 1 wpi. DC1 cells are characterized by higher surface expression of MHCII and co-stimulatory molecules than DC2 cells. We found that MHCII expression and co-stimulatory molecule expression of CD86 was decreased on the surface of DCs from anti-TNFα-treated mice relative to control mice (Figs. 2C-D). This supported our hypothesis that TNFα-depletion resulted in DC2 polarization rather than DC1, which preceded the differential polarization of T-cells.

Figure 2

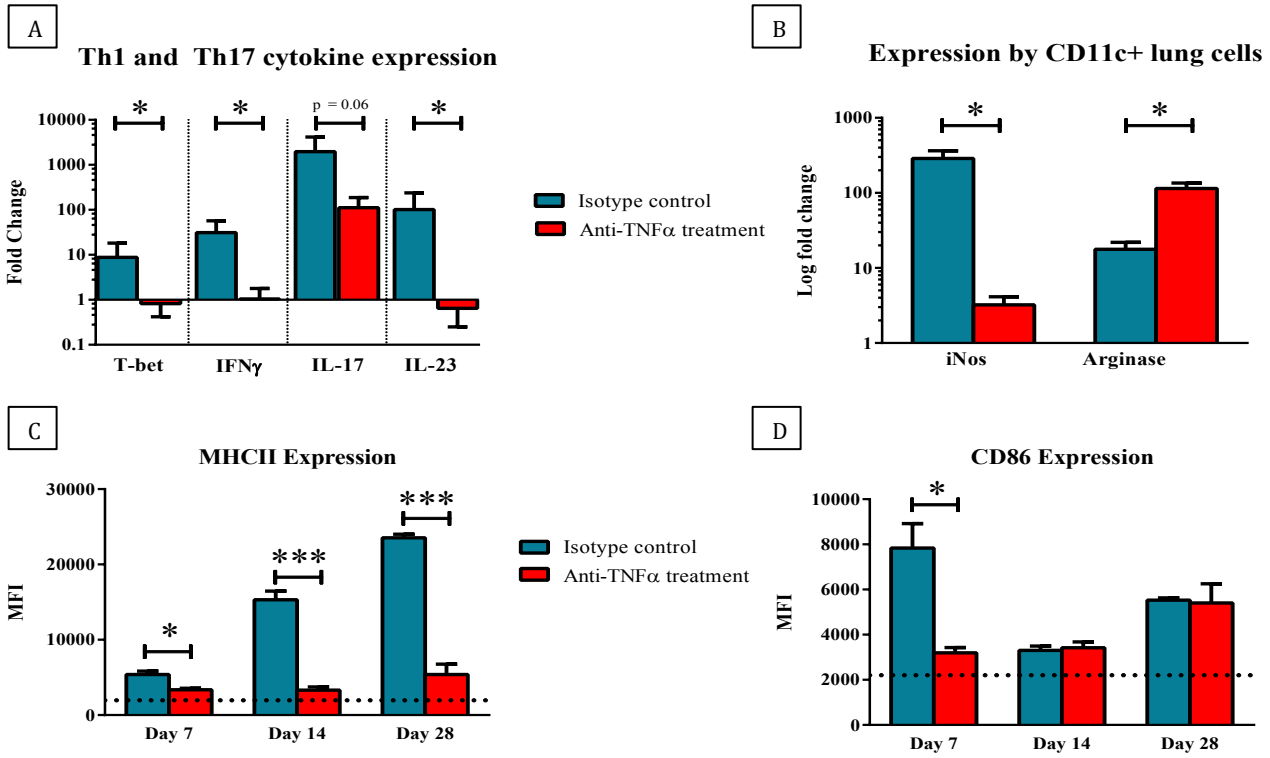

Figure 2 –Leukocytes were isolated through enzymatic digestion of whole mouse lungs from mice at indicated time points (n = 8). $CD4^+$ cells were isolated by magnetic bead separation at 2 wpi, preserved in Trizol, and levels of mRNA for various Th1 associated genes were evaluated using qPCR (Fig. 2A). $CD11c^+$ cells (primarily DCs) were isolated using magnetic bead separation and analyzed for levels of Th1 and Th2 associated signaling molecules at 2 wpi (Fig. 2B). Mean fluorescence intensity (MFI) surface staining of lung leukocyte populations and flow cytometric analysis was used to measure MHCII surface protein (Fig. 2C) or CD86 costimulatory molecule surface expression (Fig. 2D) levels of DCs from each treatment group (n = 6-8). Data represent pooled data from 2-4 separate, matched experiments. Dotted black line represents MFI of uninfected, untreated control mice. * $p < 0.05$, *** $p < 0.001$ between indicated values.

TNFα promotes lasting suppression of DC2 associated genes and stabilizes DC1 gene expression in DCs *in vivo* despite exposure to IL-4.

We next used *in vitro* methods to further explore the mechanism of DC polarization. We developed a system of cytokine cycling experiments to determine the role of TNFα on Bone Marrow-derived Dendritic Cells (BMDCs) (Fig. 3). In these experiments, BMDCs are cultured and matured for 7 days in the presence of GM-CSF, plated, and stimulated with DC1 polarizing cytokine IFNγ alone or in combination with TNFα, which comprises the "training phase." After 24 hours, the cytokine environment is either switched to the DC2 polarizing cytokine IL-4, or re-stimulated with IFNγ, for the "challenge phase."

To explore the affects of TNFα on DC polarization *in vitro*, we analyzed levels of key DC2 marker genes Gal3, Fizz1, IL-13 and DC1 marker genes iNOS and IL-12b (Fig. 4). DCs exposed to IFNγ alone or in combination with TNFα during the training phase and IFNγ alone during the challenge phase had a DC1 gene expression profile characterized by low Fizz1, low Gal3, low IL-13, high iNOS and high IL-12b. DCs stimulated with IFNγ alone and challenged with IL-4 had increased levels of Gal3, Fizz1 and IL-13 indicating a DC2 polarization. However, when DCs were stimulated with IFNγ in the presence of TNFα, DC2 gene levels remained consistent with the DC1 primary stimulation phenotype after they were challenged with IL-4. This indicated that in the absence of TNFα, DCs are unable to resist changes to their DC2 polarization.

Figure 3

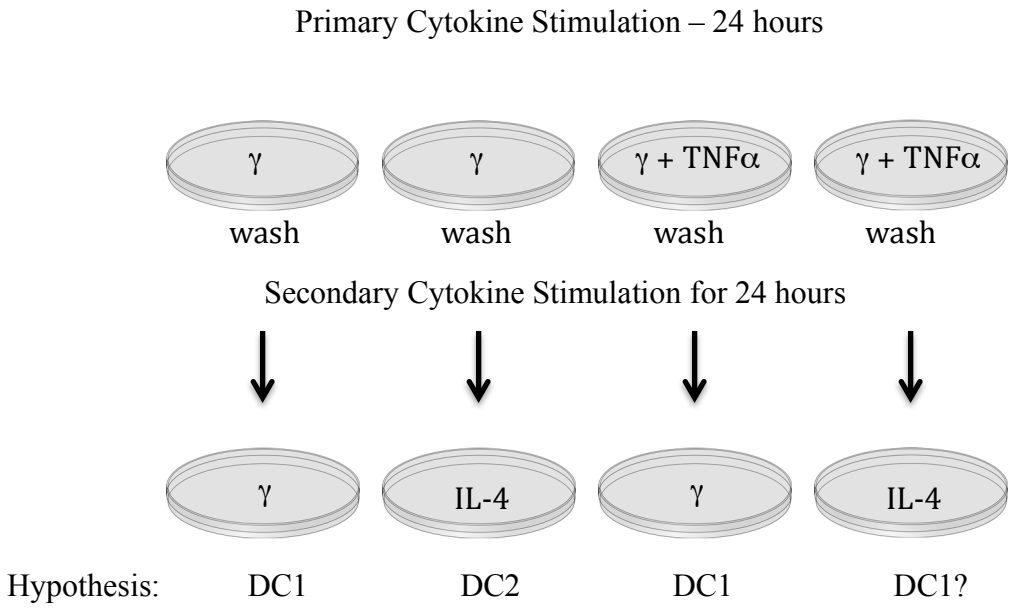

Figure 3 - Cytokine cycling experiment schematic. Bone marrow-derived dendritic cells (BMDCs) were collected from the bones of uninfected CBA/J mice and cultured over 7 days in the presence of GM-CSF to preferentially develop DCs. At day 7, the loosely-adherent fraction was harvested and plated. Cells were cultured in the indicated cytokine environments for 24 hours, washed, and given another 24-hour cytokine stimulation.

Figure 4

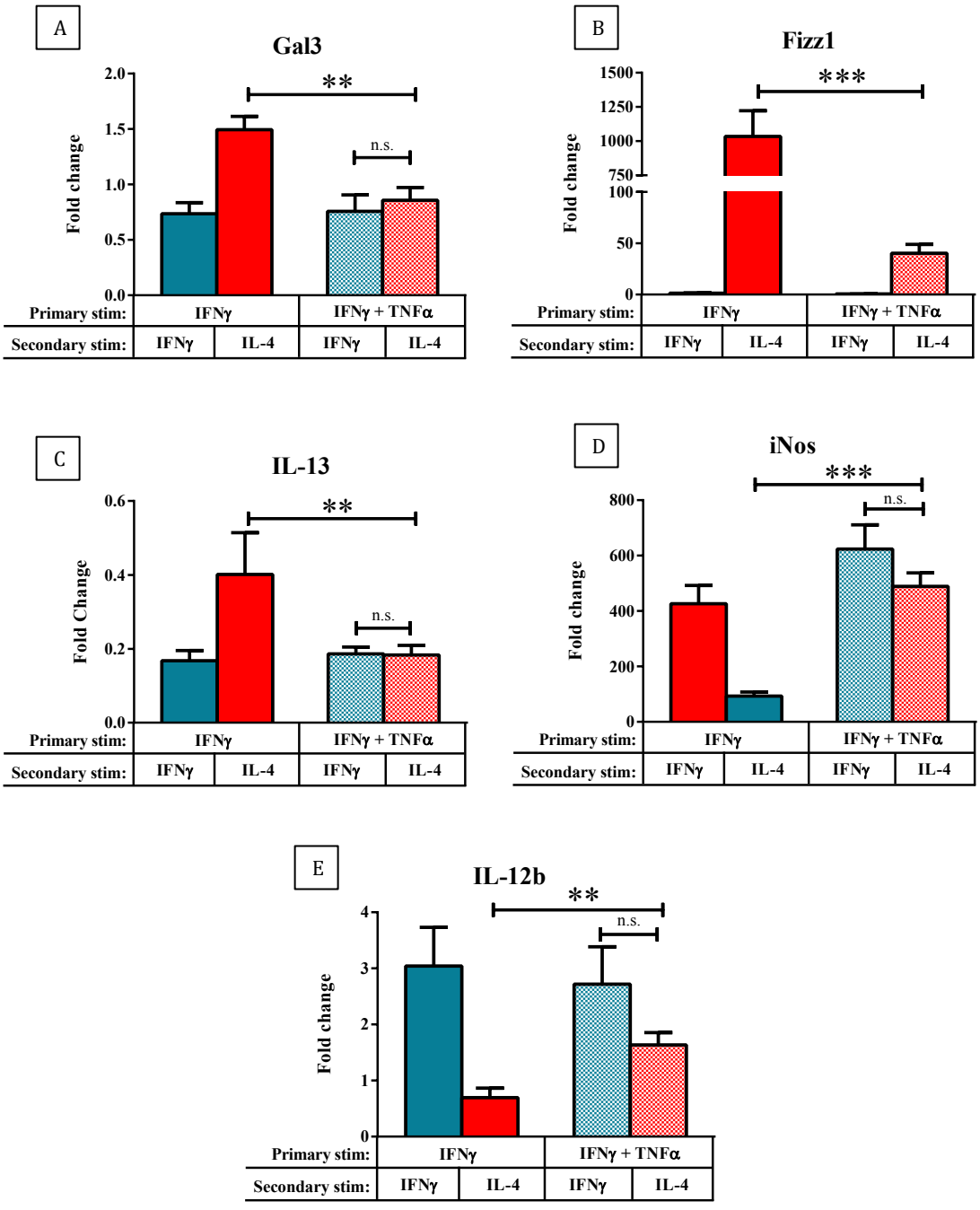
A
Gal3
Fold change
2.0
1.5
1.0
0.5
0.0
**
n.s.
Primary stim:
IFNγ
IFNγ + TNFα
Secondary stim:
IFNγ
IL-4
IFNγ
IL-4
B
Fizz1
Fold change
1500
1250
1000
750
100
50
0
***
Primary stim:
IFNγ
IFNγ + TNFα
Secondary stim:
IFNγ
IL-4
IFNγ
IL-4
C
IL-13
Fold Change
0.6
0.4
0.2
0.0
**
n.s.
Primary stim:
IFNγ
IFNγ + TNFα
Secondary stim:
IFNγ
IL-4
IFNγ
IL-4
D
iNos
Fold change
800
600
400
200
0
***
n.s.
Primary stim:
IFNγ
IFNγ + TNFα
Secondary stim:
IFNγ
IL-4
IFNγ
IL-4
E
IL-12b
Fold change
4
3
2
1
0
**
n.s.
Primary stim:
IFNγ
IFNγ + TNFα
Secondary stim:
IFNγ
IL-4
IFNγ
IL-4

Figure 4 - Cells were cultured and harvested using the above schematic. mRNA was extracted from each group and data pooled from at least 3 experiments, each with 3 wells of the same treatment group. Levels of Th2 (Gal3, Fizz1, IL-13, Figs. 4A-C) and Th1 (iNOS, IL-12b Figs. 4D-E) associated genes were analyzed using qPCR (Figs. 4A-E). * $p < 0.05$, ** $p < 0.01$, *** $p < 0.001$ between the indicated treatment groups.

Expression of repressive modification H3K27 trimethylation is increased *in vivo* upon treatment with anti-TNFα antibody.

We then proceeded to explore the epigenetic controls to key DC genes in the DC training process. To assess global epigenetic differences between DC1 and DC2 cells, we measured H3K27me3, which is a repressive modification, in lung DCs by intranuclear flow cytometry (Fig. 5A-B). Quantification of histogram results show a near-significant trend ($p= 0.052$) towards higher mean fluorescence intensity representing the repressive H3K27me3 modification in pre-DCs (monocytes) in the lungs of anti-TNFα treated mice at 1 wpi (Figs. 5C). This motivated more robust analysis of the percentage of cells highly enriched with the repressive H3K27me3 signature. Analysis revealed that TNFα depletion increased the percentage of DCs expressing high global H3K27me3 signature in *C. neoformans* infected lungs (Figs 5D-E). This signifies a difference in epigenetic modification to the H3K27 residue in the presence or absence of TNFα signaling. The increased presence of H3K27me3 in samples treated with anti-TNFα indicates the higher level of repressive epigenetic signature when the cytokine is depleted.

Figure 5

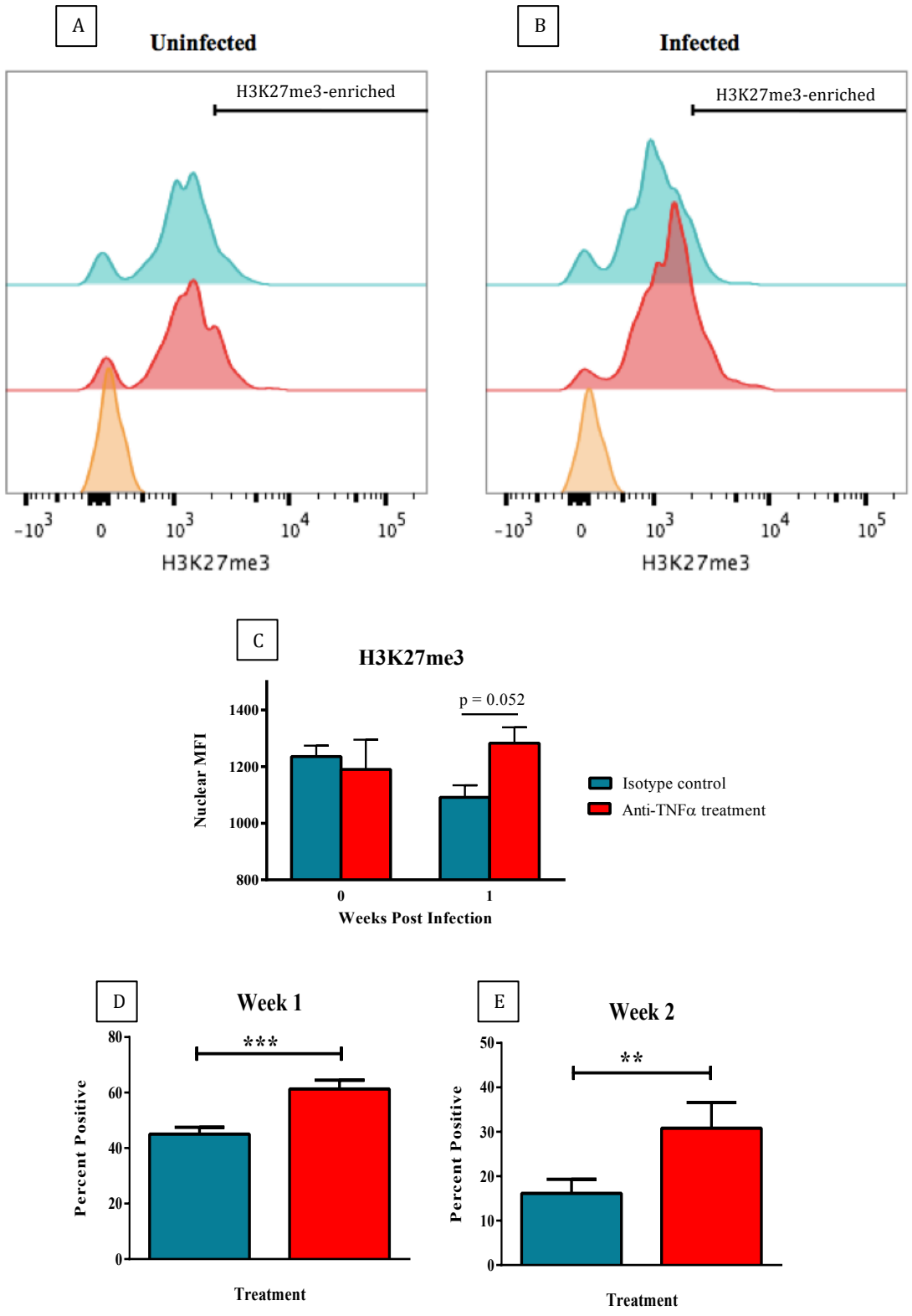
A
Uninfected
H3K27me3-enriched
-10^3
0
10^3
10^4
10^5
H3K27me3
B
Infected
H3K27me3-enriched
-10^3
0
10^3
10^4
10^5
H3K27me3
C
H3K27me3
p = 0.052
Nuclear MFI
1400
1200
1000
800
0
1
Weeks Post Infection
Isotype control
Anti-TNFα treatment
D
Week 1
***
Percent Positive
80
60
40
20
0
Treatment
E
Week 2
**
Percent Positive
50
40
30
20
10
0
Treatment

Figure 5 – Flow cytometric analysis of lung DCs at 1 and 2 wpi. Cells were fixed, permeablized, and intranuclear flow cytometry was performed for the histone modification H3K27me3. Data presented as representative histograms (Fig. 5A) and MFI (n = 6-8, Figs. 5B-C) shows that in the absence of infection, there are no substantial differences in the H3K27me3 signature of the DCs with (blue) and without (red) TNFα (yellow indicates intranucler isotype antibody staining). However, during infection, DCs in the absence of TNFα have a more pronounced H3K27me3 signature assessed by MFI (Fig. 5C) and by percent of cells with enriched H3K27me3 at multiple time points post-infection (Figs. 5D-E). ** $p < 0.01$, *** $p < 0.001$ between indicated groups.

TNFα reduces levels of gene expression of histone methyltransferase EZH2 in BMDCs, and treatment with anti-TNFα leads to upregulated expression of EZH2 upon infection *in vivo*.

Because the level of H3K27me3 was increased in DC2 polarized DCs, we assessed expression of EZH2, a major component of the PRC2 complex, which is a key H3K27 methyltransfersase *in vitro* and *in vivo*. DCs matured *in vitro* in the presence of TNFα and IFNγ had uniformly low expression of EZH2 regardless of challenge with IL-4, consistent with a DC1 phenotype; however, cells matured without TNFα (IFNγ alone) and challenged with IL-4 had an upregulation of EZH2, which correlates with the DC2 phenotype (Fig. 6A). *In vivo,* DCs from the lungs of *C. neo* infected mice that were TNFα-depleted had likewise significantly more EZH2 mRNA expression than DCs from infected control mice (Fig. 6B). This data corresponded to our H3K27me3 data, suggesting that EZH2 upregulation leads to higher methylation at H3K27, and that this happens in DC2-polarized cells.

Figure 6

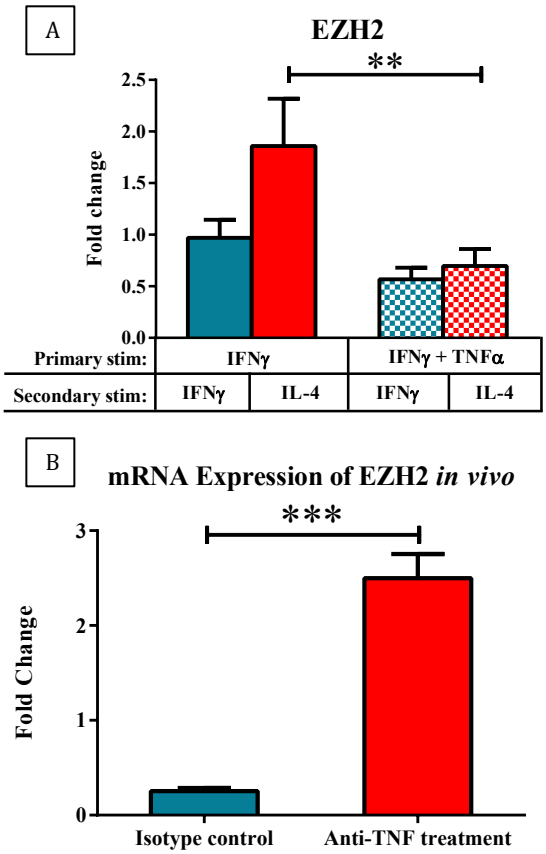

Figure 6 – BMDCs were collected from the bones of uninfected CBA/J mice. Cytokine cycling experiments were performed using the method described in Figure 3. mRNA was extracted from each group and data was pooled from 2 experiments, each with 3 wells of the same treatment group. Levels of EZH2 were analyzed using qPCR (Fig. 6A). For our *in vivo* studies, $CD11c^{+}$ cells were magnetically separated from lung leukocytes isolated from mice at 1 wpi (n = 4-8). EZH2 gene expression was evaluated using qPCR (Fig. 6B). Data represent pooled data from 3 separate, matched experiments. ** $p < 0.01$, *** $p < 0.001$ between indicated groups.

TNFα prevents repressive modification H3K27me3 at DC1 gene promoter otherwise induced by IL-4.

Because both H3K27me3 and the H3K27 methyltransferase complex were increased in cells with a DC2 phenotype, we next assessed whether the repressive H3K27me3 modification was associated with DC1 gene promoters in DC2s. We performed ChIP-PCR and using H3K27me3-specific antibodies to immunoprecipitate the histone-DNA complexes and using primers specific to the promoter region of IL-12b. We found that in cells matured *in vitro* with IFNγ that were challenged with IL-4 (phenotypically DC2 cells), there was an increase in the amount of IL-12b promoters associated with the repressive H3K27me3 (Fig. 7), indicating that the IL-12b promoter is epigenetically silenced in DC2 cells. However, DCs matured with IFNγ and TNFα that were subsequently challenged with IL-4 did not have IL-12b associated with the H3K27me3. Thus, in the absence of TNFα, DC2s have epigenetically repressed DC1 genes, but in the presence of TNFα, the IL-12b promoter becomes protected from this repression (effect associated with corresponding differences in the expression of H3K27 methyltransferase EZH2).

Figure 7

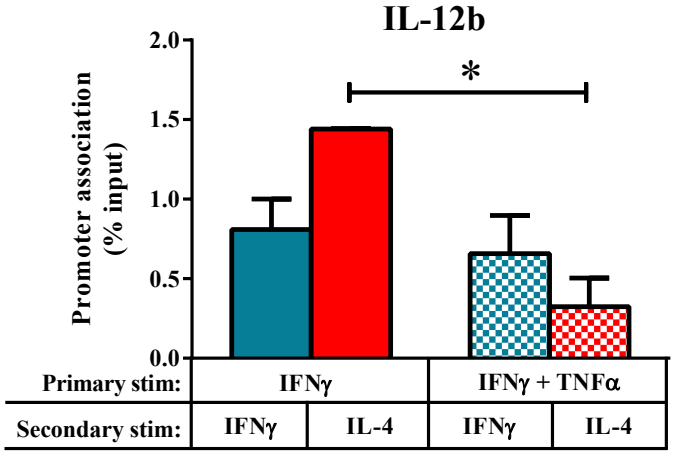

Figure 7 – BMDCs were collected from the bones of uninfected CBA/J mice. Cytokine cycling experiments were performed using the method described in Figure 3. Chromatin Immunoprecipitation Assay was performed using anti-H3K27me3 antibodies. Resulting DNA was purified and qPCR was performed using primers specific for the promoter region of IL-12b. * $p < 0.05$ between indicated groups.

Discussion

These studies have indicated that TNFα plays a crucial role in modulating epigenetic changes to H3K27 residues in DCs during fungal infection and in programming the immune response. This is the first report of this type made in a fungal infection.

TNFα depletion profoundly impaired fungal clearance during the adaptive immune response. Both lung and spleen fungal burdens were over 100-fold higher in mice treated with anti-TNFα antibodies, which depleted TNFα signaling during the early stage of infection. Our results are consistent with previous studies, which have shown that early TNFα is required for generation of the immune protection against *C. neoformans* [28-31]. Our data show the crucial role of TNFα in programming the immune response, especially in prevention of non-protective skewing to a Th2 phenotype. Serum harvested from infected mice showed that type 2 cytokines are found in significantly higher levels in infected mice depleted of TNFα as compared to mice that did not receive treatment. Because levels of IL-13 and IL-5 were significantly higher in anti-TNFα treated groups, we can see that TNFα signaling "programs" the development of the desirable type of immune response, while in its absence the immune system becomes "programmed" for development of a non-protective response. Although levels of TNFα recover, the fungal burden remains significantly lower in anti-TNFα treated mice at 2 wpi and beyond [15]. This led us to hypothesize that early TNFα could induce or prevent certain epigenetic modifications, which in turn could support or repress expression of genes responsible for the development of the desirable Th1 immunophenotype.

T-cell polarization during *C. neo* infection in the absence of TNFα was consistently skewed towards a non-protective Th2 response. TNFα depletion lead to decreased levels of Th1

associated cytokines, indicating that TNFα is necessary to prime a protective immune response. In other models of fungal infection in the absence of TNFα, including *Candida albicans, Aspergillus fumigatus,* and *Paracoccidioides bransiliensis*, neutrophils have been shown to be a critical cell population for clearance [30]. However, the effects of TNFα depletion have been shown to be independent of neutrophil action during *C. neo* infection [30]. This suggests that another mechanism occurs to boost host defenses and leads to fungal clearance of *C. neo*. We chose to explore the alternate possibility of TNFα priming of DCs in a way that enables them to orchestrate protective Th1 T-cell polarization.

Our cycling experiments show that TNFα "trains" DCs to sustain protective DC1 programming acquired during their initial stimulation with IFNγ and prevent their switch to DC2 phenotype during subsequent stimulation with the strong pro-DC2 factor, IL-4. DCs resisted DC2 gene induction after replacement of IFNγ by IL-4 only when TNFα was present during the initial stimulation. This indicates that TNFα stabilized DC1 programming induced by IFNγ, while its absence allowed DCs to remain prone to switching to DC2. Depletion of TNFα results in DCs of increased plasticity to their cytokine environments.

Our studies show that during cryptococcal infection, DCs show enhanced expression of major histocompatibility complex II (MHCII) and various co-stimulatory molecules (CD40, CD80, CD86) [49]. Mature DCs also produce a variety of cytokines (IL-12, IL-6, IL-4, IL-13, and TGF-β), which in turn program T-cell polarization [50]. Among these molecules, robust expression of MHCII and IL-12 are necessary for the priming of T-cells into Th1 cells by DCs [16-18]. Because priming of DCs into DC1s has been shown to be critical for the development of a protective Th1 response against *C. neo*, our data indicate that initial depletion of TNFα may inhibit this process [30]. Inhibition of DC1 development could be related to either delayed

maturation of DCs or the development of DC2 phenotype in place of DC1. Our data demonstrate that blocking TNFα *in vitro*, even in the absence of infection, may prime DCs towards DC2 rather than DC1. This contradicts previously postulated mechanisms for the development of immature DCs that suggest DC2 polarization by diminished expression of MHCII [14]. Diminished MHCII expression, however, may characterize both immature DCs and DC2. Our novel data (*in vitro and in vivo*) show that the absence of TNFα signaling enables upregulation of DC2 signature by DCs in addition to diminished expression of MHCII. Examination of key DC2 genes, including Gal3, Fizz1, and IL-13, demonstrates that the absence of TNFα leads to formation of DC2s. This represents a critical step in the understanding more about basic DC biology.

Because DC1s and DC2s exert differential long-term effects on host responses, we hypothesized that epigenetic gene regulation would be different between these two cell types, similar to differential epigenetic regulation observed in macrophages [51-53]. Consistent with this hypothesis, we observed higher levels of repressive modification H3K27me3 in DCs from mice that received anti-TNFα treatment as compared to untreated mice. This indicates that in the absence of TNFα, DCs from infected mice may show enhanced levels of repressive epigenetic modifications compared to mice that developed protective immune response with the help of endogenously induced TNFα. Consistently, TNFα signaling resulted in downregulation of histone methyltransferase EZH2, which is responsible for H3K27me3 (Fig. 5). Pervious work has shown that TNFα can signal to EZH2 using the MAPK pathway, specifically p38α [48]. EZH2 is being increasingly investigated for its role in cancer, and its inhibitors are currently being tested in tumor therapy [44]. Based on our studies, inhibition of EZH2 could also be

beneficial for clearance of *C. neo* infection, and we anticipate that such therapy may eventually become possible.

Our group has also explored the potential activating epigenetic modifications observed during the tri-methylated state of H3K4. Data not shown in this paper indicate that *in vitro*, levels of the H3K4 histone methyltransferase MLL1 in BMDCs increase upon addition of TNFα. Additionally, DCs isolated from the lungs of infected mice showed decreased levels of MLL1 in the absence of TNFα on day 7 post-infection. The increase in MLL1 transcript levels corresponds to increased global tri-methylation of H3K4 in the lungs of infected mice on day 7 post-infection. Because H3K4me3 is associated with gene activation [42], increased expression of MLL1 suggests that TNFα promotes the priming of DC1 through epigenetic modifications. These results fit with our hypothesis of the effects of TNFα on dendritic cells, which occur with both repressive (H3K27me3) and activating (H3K4me3) epigenetic signatures.

While global increase in H3K27me3 could affect multiple genes, we were interested in major genes involved in DC signaling that lead to successful development of type 1 immunity. IL-12 is one of the most important signals leading to the development of the protective Th1 response. Our preliminary data from *in vitro* ChIP experiments show significant enrichment of H3K27me3 at the promoter of gene IL-12b in absence of TNFα signaling. While further experiments are necessary to determine the baseline epigenetic state in DCs and how TNFα plays a role in the epigenetic regulation process *in vivo*, our *in vitro* data are consistent with notion that TNFα prevents suppressive trimethylation at the promoter region of IL-12 gene.

In summary, this work has explored the role of pro-inflammatory cytokine TNFα in the polarization of DCs in the context of infection of the opportunistic fungal pathogen,

Cryptococcus neoformans. Although extensive work has been done regarding the importance of TNFα early in infection, the exact mechanism has been poorly understood and presumed defect in DC maturation. We demonstrated that TNFα prevented detrimental DC2 polarization, interfering with the repressive epigenetic modification H3K27me3. Specifically, we have shown that in absence of TNFα, promoters of key DC1 gene IL-12b were epigenetically repressed via this motif. These data shed a light on the mechanisms by which DCs polarize upon infection, which may have broader implications for understanding mechanisms of host defenses for a wide variety of fungal pathogens and may lead to the development of therapeutic targets in the future.

Acknowledgements

This work would not have been possible without the many individuals who helped me along the way. First, I would like to thank my research mentor for the past four years, Dr. Michal Olszewski. Dr. Olszewski has helped me tremendously in providing guidance and constant support throughout my years at the University of Michigan, and by helping me realize my passion for research. He has also assisted in connecting me to multiple opportunities, including my Undergraduate Research Opportunities Program (UROP) research fellowship and the Intramural NIAID Research Opportunities Program (INRO) at the NIH. I would also like to thank my mentor in the lab, Alison Eastman. Alison has been a phenomenal help in my understanding of immunology and research as a whole. She has helped to develop experimental plans, compile my results, and troubleshoot as necessary, which has been critical to the development of this work. Additionally, I would like to thank my fellow members of the lab, including Dr. Yafeng Qiu, Antoni Malachowski, Jacob Carolan, Enze Xing and Daphne Cheng. Dr. John Osterholzer and his lab have also been instrumental in supporting my research and our experiments. Thank you to Ilona Kryczek and Steve Kunkel for assisting us with developing protocols for our experiments. I would also like to thank the UROP program for connecting me with Dr. Olszewski. Finally, thank you to my friends and family who have supported me throughout my research journey and the writing of my thesis.

References

1. Park BJ, Wannemuehler KA, Marston BJ, Govender N, Pappas PG, Chiller TM. Estimation of the current global burden of cryptococcal meningitis among persons living with hiv/aids. *AIDS* 23(4), 525-530 (2009).
2. Chuck SL, Sande MA. Infections with cryptococcus neoformans in the acquired immunodeficiency syndrome. *The New England journal of medicine* 321(12), 794-799 (1989).
3. Pappas PG, Perfect JR, Cloud GA *et al*. Cryptococcosis in human immunodeficiency virus-negative patients in the era of effective azole therapy. *Clin Infect Dis* 33(5), 690-699 (2001).
4. Velagapudi R, Hsueh YP, Geunes-Boyer S, Wright JR, Heitman J. Spores as infectious propagules of cryptococcus neoformans. *Infect Immun* 77(10), 4345-4355 (2009).
5. Cassone A, Simonetti N, Strippoli V. Wall structure and bud formation incryptococcus neoformans. *Arch. Microbiol.* 95(1), 205-212 (1974).
6. Giles SS, Dagenais TR, Botts MR, Keller NP, Hull CM. Elucidating the pathogenesis of spores from the human fungal pathogen cryptococcus neoformans. *Infect Immun* 77(8), 3491-3500 (2009).
7. Feldmesser M, Kress Y, Casadevall A. Dynamic changes in the morphology of cryptococcus neoformans during murine pulmonary infection. *Microbiology* 147(Pt 8), 2355-2365 (2001).
8. Baddley JW, Perfect JR, Oster RA *et al*. Pulmonary cryptococcosis in patients without hiv infection: Factors associated with disseminated disease. *European journal of clinical*

microbiology & infectious diseases : official publication of the European Society of Clinical Microbiology 27(10), 937-943 (2008).

9. Spitzer ED, Spitzer SG, Freundlich LF, Casadevall A. Persistence of initial infection in recurrent cryptococcus neoformans meningitis. *Lancet* 341(8845), 595-596 (1993).
10. Kobayashi M, Murata K, Hiroshi HO, Tokura Y. Cryptococcosis: Long-lasting presence of fungi after successful treatment. *Acta dermato-venereologica* 84(4), 320-321 (2004).
11. Bourgeois C, Majer O, Frohner IE, Tierney L, Kuchler K. Fungal attacks on mammalian hosts: Pathogen elimination requires sensing and tasting. *Current opinion in microbiology* 13(4), 401-408 (2010).
12. Brubaker SW, Bonham KS, Zanoni I, Kagan JC. Innate immune pattern recognition: A cell biological perspective. *Annu Rev Immunol* 33, 257-290 (2015).
13. Von Garnier C, Filgueira L, Wikstrom M *et al*. Anatomical location determines the distribution and function of dendritic cells and other apcs in the respiratory tract. *J Immunol* 175(3), 1609-1618 (2005).
14. Wozniak KL, Levitz SM. Cryptococcus neoformans enters the endolysosomal pathway of dendritic cells and is killed by lysosomal components. *Infect Immun* 76(10), 4764-4771 (2008).
15. Eastman AJ, Osterholzer JJ, Olszewski MA. Role of dendritic cell-pathogen interactions in the immune response to pulmonary cryptococcal infection. *Future microbiology* 10(11), 1837-1857 (2015).
16. Abe K, Kadota J, Ishimatsu Y *et al*. Th1-th2 cytokine kinetics in the bronchoalveolar lavage fluid of mice infected with cryptococcus neoformans of different virulences. *Microbiology and immunology* 44(10), 849-855 (2000).

17. Zhang Y, Wang F, Tompkins KC *et al*. Robust th1 and th17 immunity supports pulmonary clearance but cannot prevent systemic dissemination of highly virulent cryptococcus neoformans h99. *Am J Pathol* 175(6), 2489-2500 (2009).

18. Mody CH, Tyler CL, Sitrin RG, Jackson C, Toews GB. Interferon-gamma activates rat alveolar macrophages for anticryptococcal activity. *American journal of respiratory cell and molecular biology* 5(1), 19-26 (1991).

19. De Jong EC, Smits HH, Kapsenberg ML. Dendritic cell-mediated t cell polarization. *Springer seminars in immunopathology* 26(3), 289-307 (2005).

20. Aguirre K, Havell EA, Gibson GW, Johnson LL. Role of tumor necrosis factor and gamma interferon in acquired resistance to cryptococcus neoformans in the central nervous system of mice. *Infect Immun* 63(5), 1725-1731 (1995).

21. Murdock BJ, Huffnagle GB, Olszewski MA, Osterholzer JJ. Interleukin-17a enhances host defense against cryptococcal lung infection through effects mediated by leukocyte recruitment, activation, and gamma interferon production. *Infect Immun* 82(3), 937-948 (2014).

22. Arora S, Hernandez Y, Erb-Downward JR, Mcdonald RA, Toews GB, Huffnagle GB. Role of ifn-gamma in regulating t2 immunity and the development of alternatively activated macrophages during allergic bronchopulmonary mycosis. *J Immunol* 174(10), 6346-6356 (2005).

23. Chen GH, Mcnamara DA, Hernandez Y, Huffnagle GB, Toews GB, Olszewski MA. Inheritance of immune polarization patterns is linked to resistance versus susceptibility to cryptococcus neoformans in a mouse model. *Infect Immun* 76(6), 2379-2391 (2008).

24. Hardison SE, Ravi S, Wozniak KL, Young ML, Olszewski MA, Wormley FL, Jr. Pulmonary infection with an interferon-gamma-producing cryptococcus neoformans strain results in classical macrophage activation and protection. *Am J Pathol* 176(2), 774-785 (2010).

25. Osterholzer JJ, Surana R, Milam JE *et al*. Cryptococcal urease promotes the accumulation of immature dendritic cells and a non-protective t2 immune response within the lung. *Am J Pathol* 174(3), 932-943 (2009).

26. Benvenuti F. The dendritic cell synapse: A life dedicated to t cell activation. *Frontiers in immunology* 7, 70 (2016).

27. Sabio G, Davis RJ. Tnf and map kinase signalling pathways. *Seminars in immunology* 26(3), 237-245 (2014).

28. Huffnagle GB, Toews GB, Burdick MD *et al*. Afferent phase production of tnf-alpha is required for the development of protective t cell immunity to cryptococcus neoformans. *J Immunol* 157(10), 4529-4536 (1996).

29. Kawakami K, Qureshi MH, Koguchi Y *et al*. Role of tnf-alpha in the induction of fungicidal activity of mouse peritoneal exudate cells against cryptococcus neoformans by il-12 and il-18. *Cellular immunology* 193(1), 9-16 (1999).

30. Herring AC, Falkowski NR, Chen GH, Mcdonald RA, Toews GB, Huffnagle GB. Transient neutralization of tumor necrosis factor alpha can produce a chronic fungal infection in an immunocompetent host: Potential role of immature dendritic cells. *Infect Immun* 73(1), 39-49 (2005).

31. Herring AC, Lee J, Mcdonald RA, Toews GB, Huffnagle GB. Induction of interleukin-12 and gamma interferon requires tumor necrosis factor alpha for protective t1-cell-mediated

immunity to pulmonary cryptococcus neoformans infection. *Infect Immun* 70(6), 2959-2964 (2002).

32. Hage CA, Wood KL, Winer-Muram HT, Wilson SJ, Sarosi G, Knox KS. Pulmonary cryptococcosis after initiation of anti-tumor necrosis factor-alpha therapy. *Chest* 124(6), 2395-2397 (2003).

33. Bauman SK, Huffnagle GB, Murphy JW. Effects of tumor necrosis factor alpha on dendritic cell accumulation in lymph nodes draining the immunization site and the impact on the anticryptococcal cell-mediated immune response. *Infect Immun* 71(1), 68-74 (2003).

34. Feldman M, Taylor P, Paleolog E, Brennan FM, Maini RN. Anti-tnf alpha therapy is useful in rheumatoid arthritis and crohn's disease: Analysis of the mechanism of action predicts utility in other diseases. *Transplantation proceedings* 30(8), 4126-4127 (1998).

35. Rau R. Adalimumab (a fully human anti-tumour necrosis factor alpha monoclonal antibody) in the treatment of active rheumatoid arthritis: The initial results of five trials. *Annals of the rheumatic diseases* 61 Suppl 2, ii70-73 (2002).

36. Kohm M, Burkhardt H, Behrens F. Anti-tnfalpha-therapy as an evidence-based treatment option for different clinical manifestations of psoriatic arthritis. *Clinical and experimental rheumatology* 33(5 Suppl 93), S109-114 (2015).

37. Boulware DR, Meya DB, Bergemann TL *et al*. Clinical features and serum biomarkers in hiv immune reconstitution inflammatory syndrome after cryptococcal meningitis: A prospective cohort study. *PLoS medicine* 7(12), e1000384 (2010).

38. Huston SM, Li SS, Stack D *et al*. Cryptococcus gattii is killed by dendritic cells, but evades adaptive immunity by failing to induce dendritic cell maturation. *J Immunol* 191(1), 249-261 (2013).

39. Conaway JW. Introduction to theme "chromatin, epigenetics, and transcription". *Annual review of biochemistry* 81, 61-64 (2012).

40. Cedar H, Bergman Y. Programming of DNA methylation patterns. *Annual review of biochemistry* 81, 97-117 (2012).

41. Schwartz YB, Pirrotta V. Polycomb silencing mechanisms and the management of genomic programmes. *Nature reviews. Genetics* 8(1), 9-22 (2007).

42. Vermeulen M, Timmers HT. Grasping trimethylation of histone h3 at lysine 4. *Epigenomics* 2(3), 395-406 (2010).

43. Kohli RM, Zhang Y. Tet enzymes, tdg and the dynamics of DNA demethylation. *Nature* 502(7472), 472-479 (2013).

44. Yoo KH, Hennighausen L. Ezh2 methyltransferase and h3k27 methylation in breast cancer. *International journal of biological sciences* 8(1), 59-65 (2012).

45. Wen H, Dou Y, Hogaboam CM, Kunkel SL. Epigenetic regulation of dendritic cell-derived interleukin-12 facilitates immunosuppression after a severe innate immune response. *Blood* 111(4), 1797-1804 (2008).

46. Takeuch O, Akira S. Epigenetic control of macrophage polarization. *European journal of immunology* 41(9), 2490-2493 (2011).

47. Kuo HP, Wang Z, Lee DF *et al*. Epigenetic roles of mll oncoproteins are dependent on nf-kappab. *Cancer cell* 24(4), 423-437 (2013).

48. Palacios D, Mozzetta C, Consalvi S *et al*. Tnf/p38alpha/polycomb signaling to pax7 locus in satellite cells links inflammation to the epigenetic control of muscle regeneration. *Cell stem cell* 7(4), 455-469 (2010).

49. Syme RM, Spurrell JC, Ma LL, Green FH, Mody CH. Phagocytosis and protein processing are required for presentation of cryptococcus neoformans mitogen to t lymphocytes. *Infect Immun* 68(11), 6147-6153 (2000).

50. Bauman SK, Nichols KL, Murphy JW. Dendritic cells in the induction of protective and nonprotective anticryptococcal cell-mediated immune responses. *J Immunol* 165(1), 158-167 (2000).

51. Foster SL, Hargreaves DC, Medzhitov R. Gene-specific control of inflammation by tlr-induced chromatin modifications. *Nature* 447(7147), 972-978 (2007).

52. Xie L, Liu C, Wang L *et al*. Protein phosphatase 2a catalytic subunit alpha plays a myd88-dependent, central role in the gene-specific regulation of endotoxin tolerance. *Cell reports* 3(3), 678-688 (2013).

53. Lyn-Kew K, Rich E, Zeng X *et al*. Irak-m regulates chromatin remodeling in lung macrophages during experimental sepsis. *PloS one* 5(6), e11145 (2010).